26th International Congress of Mechanical Engineering
COBEM 2021
ABCM Associação Brasileira de Engenharia e Ciências Mecânicas
November 22-26, 2021, Virtual Congress, Brazil

COB-2021-1875- MODELING OF AN EXPERIMENTAL SETUP OF AN ELECTROMECHANICAL SYSTEM THROUGH LINEAR AND NONLINEAR SYSTEM IDENTIFICATION

Leonardo Dias Pereira[1,2]
[1]Centro Universitário Augusto Motta (UNISUAM)
Av. Paris, 84 - Bonsucesso, Zip code 21041-020, Rio de Janeiro, RJ, Brazil
leonardo.diaspereira@souunisuam.com.br
Lara Candido Alvim[2]
Helon Vicente Hultmann Ayala[2]
Hans Ingo Weber[2]
[2]Department of Mechanical Engineering, Pontifical Catholic University of Rio de Janeiro (PUC-Rio)
Marques de Sao Vicente, 225 - Gávea, Zip code 22453-900, Rio de Janeiro, RJ, Brazil
laracalvim@aluno.puc-rio.br
helon@puc-rio.br
hans@puc-rio.br

Abstract. *The present work investigates the data-driven modeling of an electromechanical system with three degrees of freedom (3-DOF), that represents a test rig setup consisting of a slender structure subjected to torsional oscillations. It is proposed to identify system parameters using benchmark datasets of test rig setup with linear approximations and, additionally, nonlinear approaches. Three model structures are applied to the system for comparative purposes. First, the linear Black-box models are the AutoRegressive with eXogenous input (ARX) and the AutoRegressive Moving Average with eXogenous input (ARMAX), then, the last one is the Nonlinear AutoRegressive Moving Average with eXogenous input (NARMAX). Finally, the modeling is validated based on a comparison made between the results obtained through One-Step-Ahead and Free Run prediction models, and the actual data acquired was considered for this purpose. This work shows the results through correlation tests and presents the best model structure based on parameters variation and R2.*

Keywords: *system identification, test-rig setup, ARX, ARMAX, NARMAX.*

1. INTRODUCTION

One of the most complex dynamical systems in industrial activities is the rotating machine. Studying the behavior of rotating machinery in the context of drilling oil wells has always been challenging in terms of increased safety, improved performance, and reduced costs.

These activities are by far the most expensive and dangerous in the entire lifecycle of the oil industry and therefore require special attention to fully understand, model and control rotating machinery. A great example of the severity of this problem can be observed in oil well drilling systems, such as stick-slip phenomena caused by torsional vibration in the drill string, as presented by Cayre (2018) and Pires (2019). The system has nonlinearities that are not easy to model and can generate complex dynamic behaviors that linear identification models can fail to accurately predict. This creates the need for non-linear system identification, which can be done through black box models.

According to Schoukens (2019), black-box models are an efficient tool to model, analyze and study dynamical systems. Through the analysis of input and output experimental data samples, these models allow the identification and modeling of system behavior.

Billings (2013) defined Nonlinear Autoregressive Moving Average Modeling with Exogenous Inputs (NARMAX) is part of the black box methods commonly used for system identification. NARMAX is used to obtain the characteristics of a non-linear system through a set of parameters. Noël (2017) presents this model as an application tool for large systems and emphasizes its complexity when considering the dimensions of the system.

Schoukens (2019) considers the AutoRegressive model with exogenous input (ARX) as the simplest method in the set of black box models. This method evaluates system output as a combination of past inputs and outputs. Differently from the NARMAX method, the ARX is specifically used for analyzing linear systems.

Jing (2021) mentioned that the AutoRegressive Moving Average with eXogenous input (ARMAX) model is also applied for modeling industrial systems, but unlike the ARX model, it includes stochastic dynamics in its analysis. This model is useful for systems with input disturbances.

Hence, in this study the main objective is to model the dynamics of a 3 DOF electromechanical system that simulates the drilling process. The purpose is to obtain a model for representing the fast dynamics which these devices may achieve by testing and comparing linear (ARX and ARMAX) and nonlinear (NARMAX) black-box models.

The remainder of this paper is organized as follows. Section 2 presents the equations of motion and experimental setup of the electromechanical system. Section 3 presents the equations of ARX, ARMAX, and NARMAX models. The results for ARX, ARMAX and NARMAX methods are compared in Section 4. Section 5 provides the conclusions and points out open questions for future work.

2. EXPERIMENTAL SETUP

2.1 Mathematical Model

This study shows the grey-box modelling of a reduced scale test rig to emulate the drill-string dynamics. The test rig is described by a nonlinear three degrees of freedom model according to Figure 1. The experiment consists of an electromechanical system subjected to a voltage as input signal u_m. The angular displacement and velocity of the three inertias $y_m(\dot{\theta}_1, \dot{\theta}_2, \dot{\theta}_3)$ are the output signal. The modeling and equations of motion of the experiment detailed below are based on the work of Cayres (2018) and Pires (2019). Therefore, the structure of the nonlinear state space model is:

$$
\begin{gathered}
J_1\ddot{\theta}_1 + d_1(\dot{\theta}_1 - \dot{\theta}_2) + k_1\delta_{12} + T_{r_1}(\dot{\theta}_1) = 0 \\
J_2\ddot{\theta}_2 + d_1(\dot{\theta}_2 - \dot{\theta}_1) + d_2(\dot{\theta}_2 - \dot{\theta}_3) + k_2\delta_{23} - k_1\delta_{12} + T_{r_2}(\dot{\theta}_2) = 0 \\
d_2(\dot{\theta}_3 - \dot{\theta}_2) - k_2\delta_{23} = \eta(K_T i - C_m\eta\dot{\theta}_3 - T_f - J_m\eta\ddot{\theta}_3) \\
L \cdot di/dt \; + Ri + K_E\eta\dot{\theta}_3 = u_m
\end{gathered} \tag{1}
$$

where i is the electrical current, L and R are the inductance and resistance, respectively. θ_m is the angular velocity of the inertia J_m. C_m and K_T are the torsional damper and the motor torque constant, respectively. K_E is the tension constant and T_f is the internal friction torque. J_i for i=1,2 is the moment of inertia of discs. The relations between the subsystems are given by $\tau_s = \eta\tau_m$ and $\dot{\theta}_m = \eta\,\dot{\theta}_3$. $\delta_{12} = \theta_1 - \theta_2$ and $\delta_{23} = \theta_2 - \theta_3$. k_1 and k_2 are the spring constants, just as d_1 and d_2 are the damping constants.

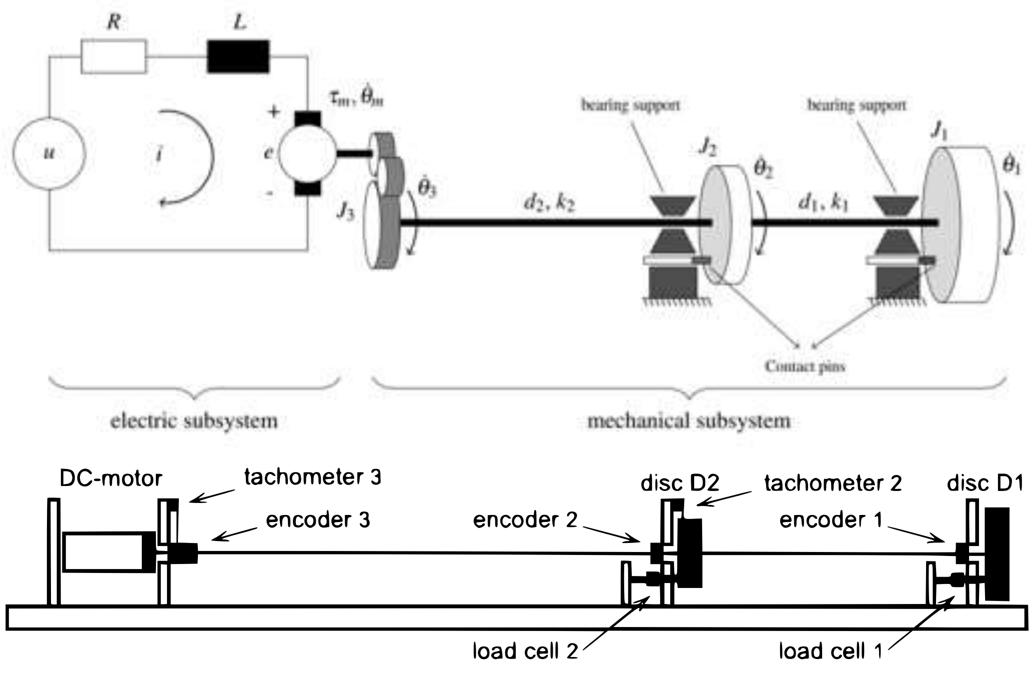

Figure 1. Schematic design of the dynamical system and Measurement setup. (Adapted from Pires, 2019).

2.2 Available Data Sets

The data set used in this work is provided by Ms. Ingrid Pires (Pires, 2018) and Mr. Walisson Pinto (Pinto, 2020) who performed the experiments in a laboratory of PUC-Rio. The data set (input and output) is recorded by the National Instruments cDAQ system and resampled with Matlab®R2020a to obtain a regular sampled frequency. The input u(t) is the voltage [V] and the output y(t) is the angular velocity [rad/s] of encoder 3 (see Figure 1). After resampling, the data set is left with 8,000 data samples, shown in Figure 2, for all estimation and validation tasks performed in this study.

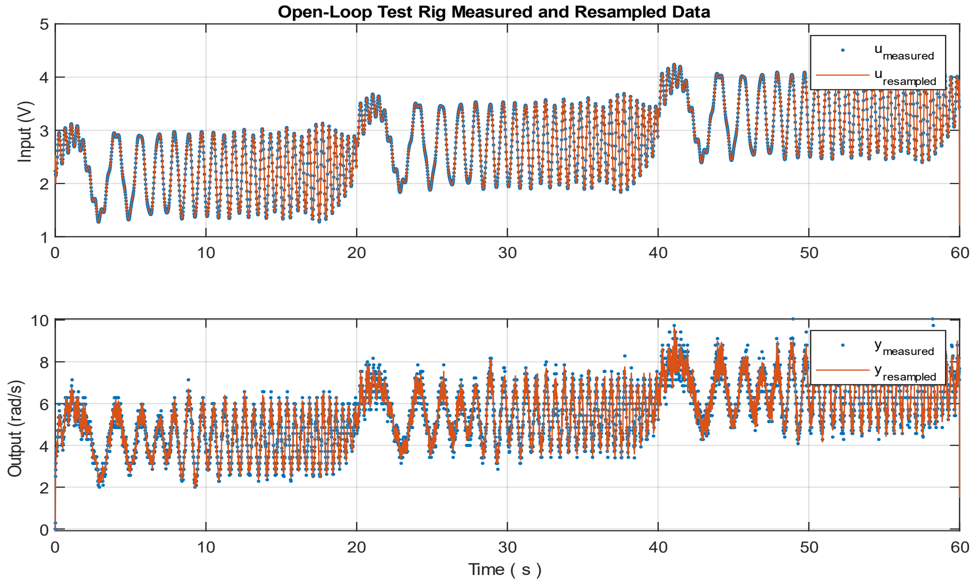

Figure 2. Comparison of the time history of the input and output measured and resampled data sets

Then, after removing the initial transient of the data, the available data set is splitted into estimation and validation, with 1500 samples each.

3. General Methodology

3.1 Identification Procedures

The identification procedure consists of a series of basic steps, and the development of each one influences the efficiency of the tested model. These steps facilitate the organization of the analysis as well as the review of the processes in case of rework. Based on this, the identification procedure is summarized as follows:

Step 1: Design the experiments to obtain information about the system and provide the input and output data.
Step 2: Choose within the mathematical models which can be applied to model the structure representing the system.
Step 3: Estimate the parameters of the model to adapt it as well as possible to the system data.
Step 4: Validate the chosen model and test whether it correctly describes the modeling of the available data.

The system identification procedure illustrated in Figure 3, is used to estimate, and predict the system parameters based on the chosen approaches for estimation and validation data sets.

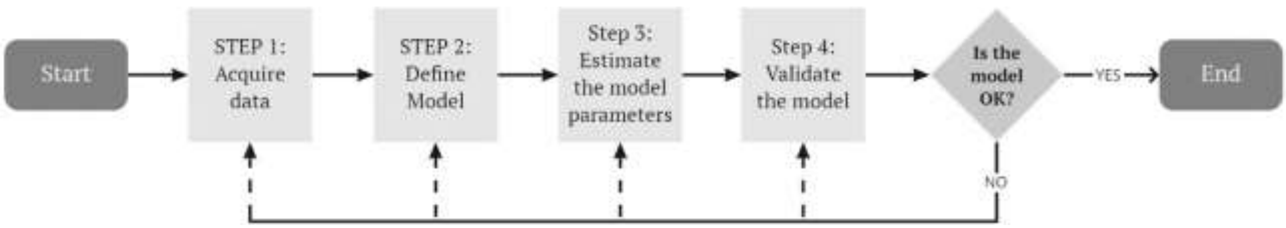

Figure 3. Diagram of the System identification procedure. (Adapted from Ayala *et al.*, 2018)

3.2 Model Structure Representation

Now, the three model structures considered for the identification process are ARX, ARMAX and NARMAX. According to Billings (2013), the ARMAX model, including subsets of AR, ARMA and ARX model, are the most frequently used representation for the identification of linear systems or whose inherent behavior can be characterized by a linear approximation close to a system operating point.

The ARX model structure is given by the equations:

$$y(k) + a_1 y(k-1) + \cdots + a_{n_a} y(k-n_a) = b_1 u(k-1) + \cdots + b_{n_b} u(k-n_b) + \xi(k), \quad (2)$$

And the ARMAX model structure is defined as:

$$y(k) + a_1 y(k-1) + \cdots + a_{n_a} y(k-n_a) = b_1 u(k-1) + \cdots + b_{n_b} u(k-n_b) + \xi(k) + c_1 \xi(k-1) + \cdots + c_{n_c} \xi(k-n_c), \quad (3)$$

where $u(k)$ and $y(k)$ $(k = 1,2,\dots,N)$ are sampled observations of input and output, n_a is output order in ARX, n_b is input order in ARX and n_c is the moving average (MA) order

The NARMAX models are the most popular representations for nonlinear dynamic system identification in the discrete-time domain (Billings,2013). This model is an expansion of past inputs, outputs, and noise terms as expressed in:

$$y(k) = F[y(k-1), y(k-2), \dots, y(k-n_y), u(k-d), u(k-d-1), \dots, u(k-d-n_u), \dots, \dots, e(k-1), e(k-2), \dots, e(k-n_e)] + e(k), \quad (4)$$

where $y(k)$, $u(k)$, and $e(k)$ are the system output, input, and noise sequences, respectively; n_y,n_u, and $n_e$are the maximum lags for the system output, input, and noise. $F[\cdot]$ is some nonlinear function, and d is a time delay typically set to $d = 1$ (Billings, 2013).

3.3 Validation Methods

The final step in system identification is the model validation. This is a very important step to define whether the model fits the data for the intended use without any bias (Zakwan et al., 2017). In this paper, two validation approaches are considered: model predicted output (MPO) and correlation tests. First, the MPO validation tests are done by comparing the simulated with the measured data. Then, the multiple correlation coefficient tests (R^2) indicate the adequacy of the model. Both validation tests are performed for the One Step Ahead (OSA) and the Free Run (FR) prediction simulation.

The OSA and FR prediction algorithms are performed for the estimation and validation data sets to predict ϕ and $\hat{y}$. Using the data points, a structure model was deliberately fitted to yield the identified model. The concept of one step ahead OSA prediction can be explained in Billings (2013, p.124).

The OSA prediction is calculated as in Eq. (5), by using the recent measured data and the Free-Run (FR) simulation, with past values predicted from the model, (Ayala *et al*., 2018).

$$\hat{y}(k) = F[y(k-1), y(k-2), \dots, y(k-n_{y_1}), u_1(k-1), u_1(k-2), \dots, u_1(k-n_{u_1}), \dots, u_2(k-1), u_2(k-2), \dots, u_2(k-n_{u_2}), \dots, u_j(k-1), u_j(k-2), \dots, u_j(k-n_{u_j})] \quad (5)$$

where $\hat{y}(k)$is the OSA predicted output.

The residual analysis is performed to verify if all the model characteristics have been captured and fitted. This validation method is applied to confirm that there is no predictable information in the residuals, Billings (2013). The residual $\xi(k)$ is given by Eq.(6).

$$\xi(k) = y(k) - \hat{y}(k) \quad (6)$$

The Multiple Correlation Coefficient (R^2) is used to measure the accuracy of the model through the residuals. If R^2 = 1, the data were reconstructed perfectly. However, $R^2 > 0.9$ is considered good enough for most cases. The R^2 coefficient is given by the Eq. (7), (Ayala *et al*., 2018).

$$R^2 = 1 - \frac{\sum_{k=1}^{N} [\xi(k)^2]}{\sum_{k=1}^{N} [y(k) - \hat{y}(k)]^2}, \quad (7)$$

Billings (2013) presents a set of correlation tests for input and output models that can be used to verify nonlinear models. In Eq. (8) the linear and nonlinear correlations of the inputs and outputs that must be respected for the residual model to be unpredictable are presented.

$$\begin{aligned}&\boldsymbol{\phi}_{\xi\xi}(\tau) = \delta(\tau),\ \forall\tau\\ &\boldsymbol{\phi}_{u\xi}(\tau) = 0,\quad \forall\tau\\ &\boldsymbol{\phi}_{\xi(\xi u)}(\tau) = 0,\quad \tau \geq 0\\ &\boldsymbol{\phi}_{(u^2)'\xi}(\tau) = 0,\quad \forall\tau,\\ &\boldsymbol{\phi}_{(u^2)',\xi^2}(\tau) = 0,\ \forall\tau,\end{aligned} \tag{8}$$

where $\phi$is the cross-correlation function, $\phi_{\xi\xi}$ and $\phi_{u\xi}$ tests are the linear combination, $\phi_{\xi(\xi u)}$,$\phi_{(u^2)'\xi}$ and$\phi_{(u^2)',\xi^2}$ tests are the nonlinear combinations.To analyze if the conditions have met and if the model is validated, plots with 95% confidence bands are created.

4. RESULTS

The present section describes the results when applying the system identification methodology based on steps 3 (estimation) and 4 (validation), as mentioned above. Both steps are performed by varying the model parameters n_a, n_b, n_c, l, $\rho_n$and ρ_p, so the best order in each case can be achieved. If linear models do not provide satisfactory results, the results provide a basis for exploring nonlinear models, then this study starts by applying linear models ARX and ARMAX and ends up using the NARMAX model with the information previously advised, according to the Table 1

Table 1 - Simulated cases varying parameter orders related to each system identification model.

Model	**ARX**			**ARMAX**			**NARMAX**		
Cases	**1**	**2**	**3**	**4**	**5**	**6**	**7**	**8**	**9**
Param. Model order	n_a=9 n_b=5	n_a=12 n_b=5	n_a=12 n_b=6	n_a=12 n_b=6 n_c=3	n_a=18 n_b=9 n_c=9	n_a=29 n_b=9 n_c=10	n_a=7 n_b=6, n_c=1 l=2 ρ_p=1·10⁻⁴ ρ_n=1·10⁻⁴	n_a=12 n_b=1 n_c=1 l=2 ρ_p=1·10⁻⁴ ρ_n=1·10⁻⁴	n_a=16 n_b=1 n_c=1 l=2 ρ_p=1·10⁻⁴ ρ_n=1·10⁻⁴

The results are analyzed in terms of the time history comparison between the OSA, FR, and measured data, as shown in Figures 5, 7, 8, and 10. Also, the statistical validation tests based on correlation as in (4) are performed, as shown in Figures 6, 9, and 11. Finally, the R^2metrics, as in (7), is shown in Table 2.

First, the ARX model as in Eq. (2) is used to estimate the model parameters by performing numerical simulation using MATLAB software based on the least squares (LS) algorithm (Billings, 2013). The algorithm permits to vary model orders n_a, n_b to improve the terms of R^2. Figures 5 and 6 illustrate the time domain and correlation tests, respectively, comparing the OSA, FR and measured data. It is possible to verify that the model is statistically invalid in relation to the tests in (8). This shows that the autocorrelation of the residuals $\phi_{\xi\xi}$ and the nonlinear term $\phi_{\xi(\xi u)}$ are all well outside the 95% confidence bands, suggesting that the system dynamics present in the data are not adequately captured by the model.

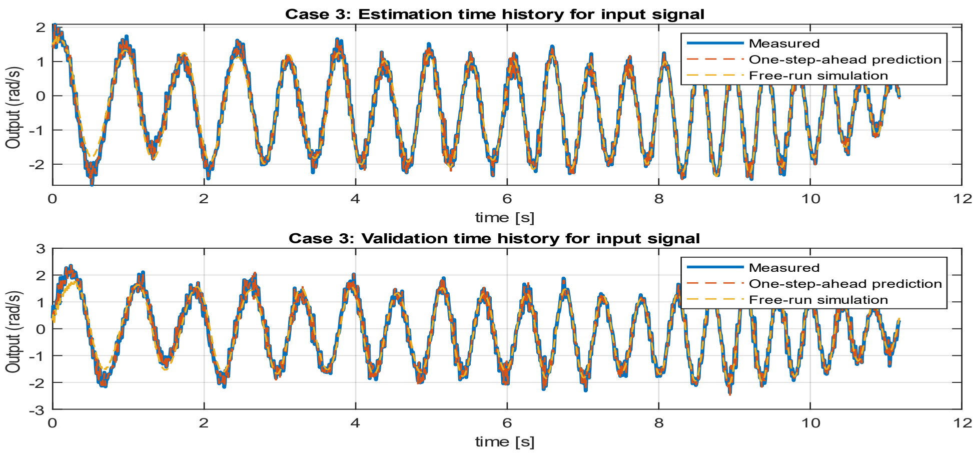

Figure 5 - Plots of OSA and FR estimation response for ARX model (Case 3).

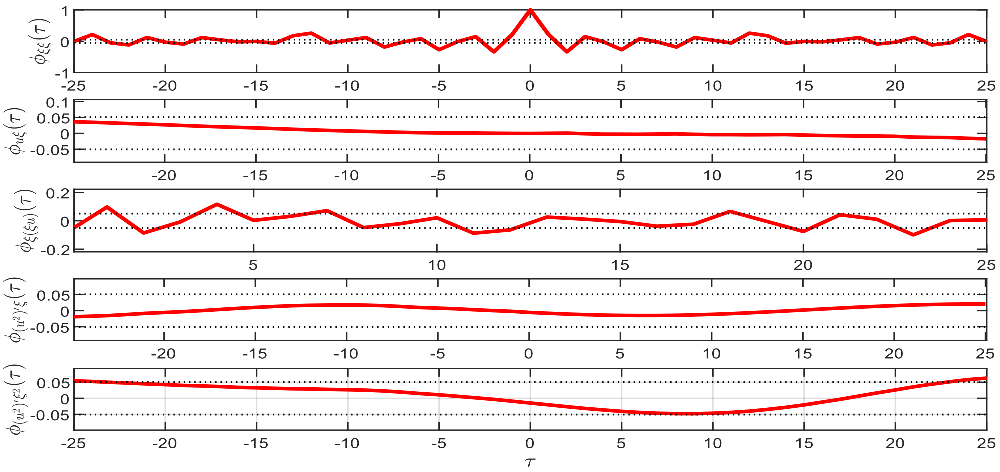

Figure 6 - Correlation tests of the inputs and outputs for ARX model (Case 3).

The ARMAX linear model as in Eq. (3) is used to calculate the moving average of linear parameters (n_a, n_b) and of the noise error n_c terms based only on the output measurements. The numerical simulation of ARMAX is performed in R software based on the extended least squares (ELS) algorithm (Billings, 2013). Figures 7 to 9 show the results of the estimation and validation in the time domain and the correlation tests for the ARMAX best case. As noted, the model still shows that the autocorrelation of the residuals $\phi_{\xi\xi}$ and the nonlinear term $\phi_{\xi(\xi u)}$ are outside the 95% confidence bands, suggesting that the system dynamics have not yet been adequately captured by the model.

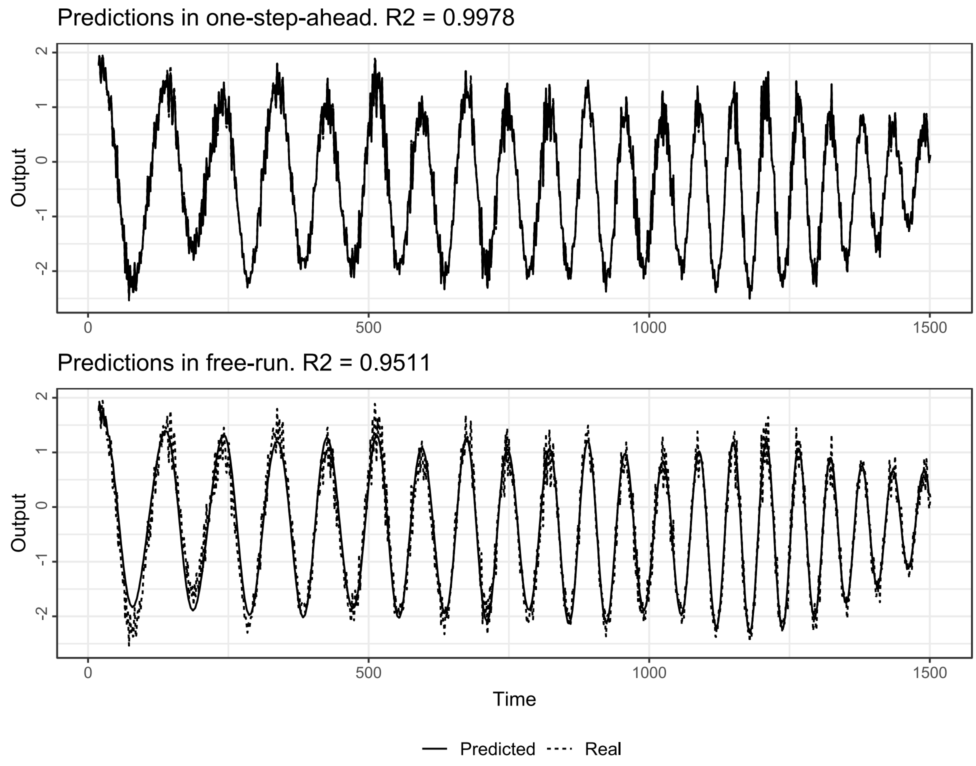

Figure 7 - Plots of OSA and FR estimation response for ARMAX model (Case 5).

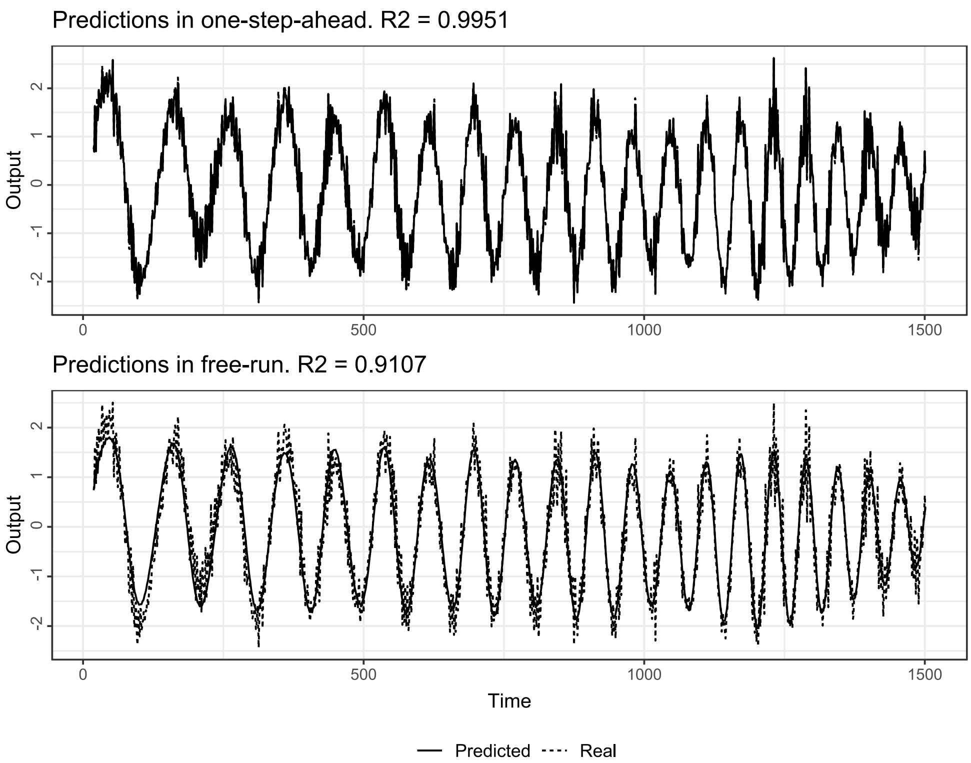

Figure 8 - Plots of OSA and FR validation response for ARMAX model (Case 5).

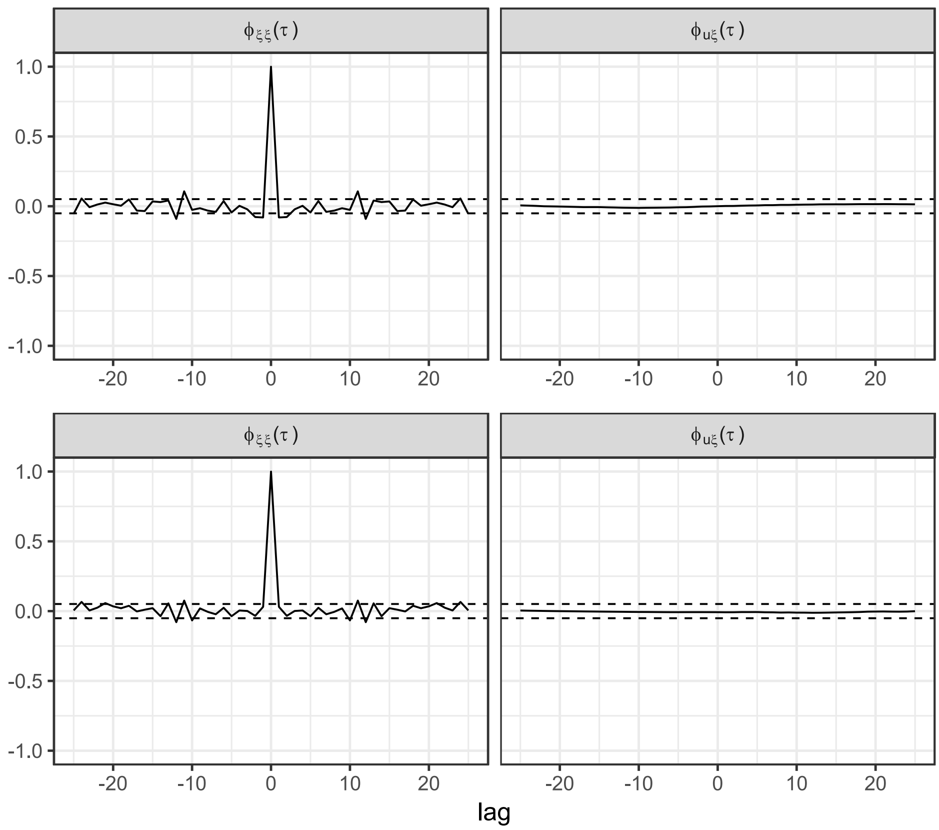

Figure 9 - Correlation tests of estimation and validation data for ARMAX model. (Case 5).

Identification of the linear model reveals that the ARX and ARMAX models provided greater than 99% fit for the estimation data and greater than 90% fit for the validation data, indicating very good fits. However, the correlation tests in both cases fail for the nonlinear term $\phi_{(u^2)', \xi^2}$. Therefore, an effort to achieve better results is to explore the Nonlinear

ARMAX (NARMAX) model as in Eq. (4). The numerical simulation of the NARMAX model is also performed in R software based on the direct regression algorithm Orthogonal Least Squares (FROLS) (Billings, 2013). Figures 10 - 11 show the results of the time domain estimation and validation and the correlation tests for the NARMAX best case. Note that the model only shows inconsistency in the nonlinear term $\phi_{(u^2)',\xi^2}$ which are outside the 95% confidence bands, suggesting that the system dynamics is almost fully captured by the model structure.

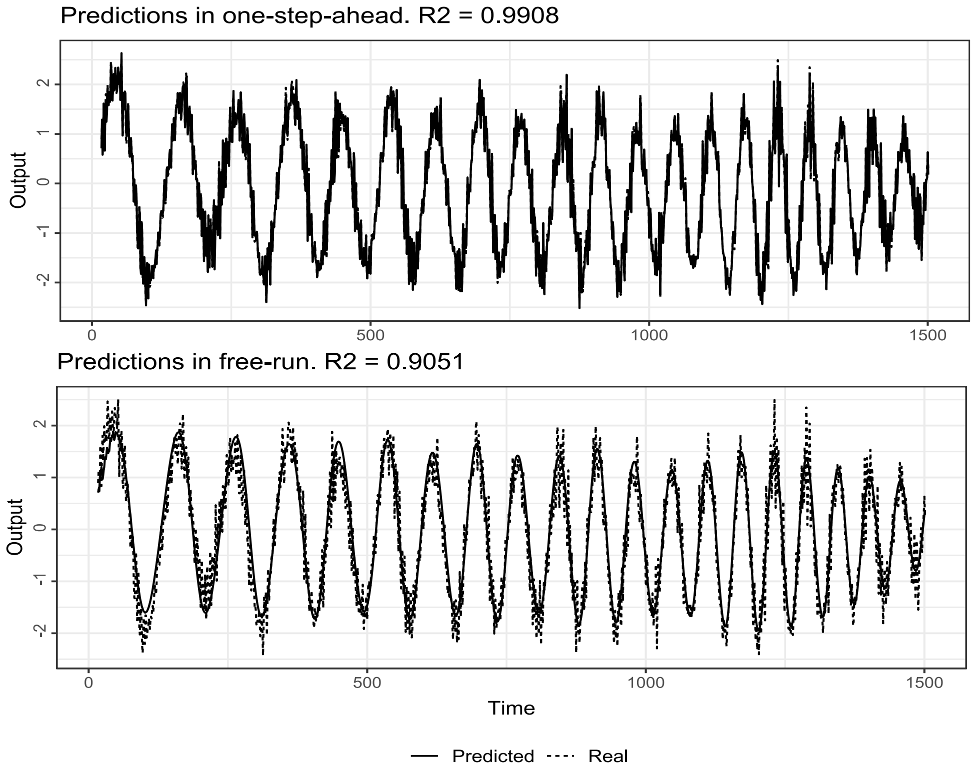

Figure 10 - Plots of OSA and FR validation response for NARMAX model (Case 9).

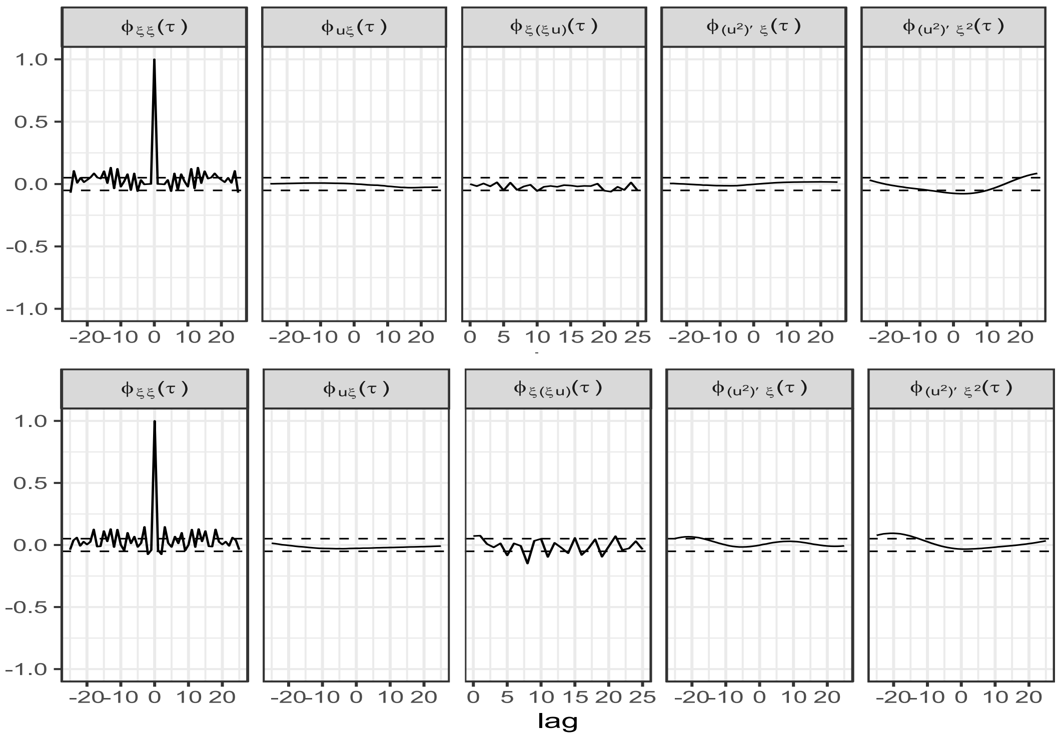

Figure 11 - Correlation tests of estimation and validation data for ARMAX model (Case 9).

Table 2 presents a summary of the best results for R^2in OSA and FR simulation and the NARMAX model is the best model to capture full systems dynamics.

Table 2 - The best R^2in OSA and FR simulation results.

Model Structure	**Cases**	**OSA**		**FR**	
		R^2_{TRA}	R^2_{VAL}	R^2_{TRA}	R^2_{VAL}
ARX	**1**	0.9928	0.9831	0.9459	0.9036
	2	0.9954	0.9819	0.9518	0.9091
	3	0.9954	0.9820	0.9516	0.9087
ARMAX	**4**	0.9971	0.9934	0.9504	0.9106
	5	0.9978	0.9951	0.9511	0.9107
	6	0.9978	0.9952	0.9494	0.9102
NARMAX	**7**	0.9943	0.9785	0.9449	0.9020
	8	0.9970	0,9898	0.9506	0.9024
	9	0.9977	0.9908	0.9516	0.9051

5. CONCLUSION

This study shows that the identification problem becomes more challenging if the output signal $y_m(\dot{\theta}_1, \dot{\theta}_2, \dot{\theta}_3)$ used for identification is physically separated from the electrical subsystem, which means that it has more influence on the mechanical subsystem. In any case, the linear model approach proved to be insufficient to capture the entire dynamic behavior of the system.

Therefore, it can be concluded that the system dynamics was well estimated by the study presented. Mainly, if the entire system identification procedure presented is considered. The procedure achieves the objective of evaluating different model structures with increasing model complexity and comparing the results to choose the best one. The system was well characterized by the NARMAX model approach. The NARMAX model, represented by case 8, fits the model well, as can be seen from the OSA estimate and the FR prediction model. Thus, for future works, many types of model structures available to approximate the unknown mapping (Neural network, Fuzzy Logic-Based Models, Wavelet Expansions) will be considered. Also, the study of the frequency domain system identification using nonparametric noise models and periodic excitations and its comparison with the time domain prediction error framework.

6. ACKNOWLEDGMENT

The authors gratefully acknowledge that the study was supported by the Department of Mechanical Engineering, Pontifical Catholic University of Rio de Janeiro.

7. REFERENCES

Åström, K. J. and Wittenmark, B. Computer-controlled Systems. Prentice-Hall, Inc., Upper Saddle River, NJ, USA, 3rd edition, 1997.

Ayala, H. V. H., Gritti, M. C., Coelho, L. S., 2020. "An R library for nonlinear black-box system identification". SoftwareX, vol. 11

Ayala, H. V. H., Rakotondrahe, M., and Coelho, L. d. S., 2018. "Modeling of a 2-DOF Piezoelectric Micromanipulator at High Frequency Rates through Nonlinear Black-box System Identification," 2018 Annual American Control Conference (ACC), pp. 4354-4359.

Billings, S. A., 2013. "Nonlinear system identification : NARMAX methods in the time, frequency, and spatio-temporal domains". SPi Publisher Services, Pondicherry, India.

Cayre, B. C., 2018. “Nonlinear dynamic analysis of dry friction-induced torsional vibration in a drill-string experimental set-up”. Doctorate’s Thesis, Department of Mechanical Engineering, Pontifical Catholic University of Rio de Janeiro. Rio de Janeiro, Brazil.

Jing, S. "Identification of an ARMAX model based on a momentum-accelerated multi-error stochastic information gradient algorithm," 2021 IEEE 10th Data Driven Control and Learning Systems Conference (DDCLS), 2021, pp. 1274-1278, doi: 10.1109/DDCLS52934.2021.9455685.

Lataire, J., Louarroudi, E., Pintelon, R., & Rolain, Y., 1999. “Benchmark data on a linear time-and parameter-varying system.” In 17th IFAC symposium on system identification, (pp. 1477–1482), Beijing, China, 2015.

Ljung, Lennart. “System identification: theory for the user”. Prentice-hall, Upper Saddle River, NJ, USA, 2 edition.

Noël, J. P., Kerschen, G. “Nonlinear system identification in structural dynamics: 10 more years of progress”. Mechanical Systems and Signal Processing, Volume 83, 2017, Pages 2-35, ISSN 0888-3270, https://doi.org/10.1016/0j.ymssp.2016.07.02.

Schoukens, J., Ljung, L. "Nonlinear System Identification: A User-Oriented Road Map" in IEEE Control Systems Magazine, vol. 39, no. 6, pp. 28-99, Dec. 2019, doi: 10.1109/MCS.2019.2938121.

Oliver Nelles., 2001. “Nonlinear system identification: from classical approaches to neural networks and fuzzy models”. Springer, Berlin, Germany, 1 edition

Padilla, A. “Recursive identification of continuous-time systems with time-varying parameters”. Automatic. Université de Lorraine, 2017.

Pinto, W. C. F., Ayala, H. V. H., 2020. “Ensemble Grey and Black-box Nonlinear System Identification of a Positioning System” in Anais do XXIII Congresso Brasileiro de Automática vol 2, no 1.

Pereira, L. D., Cayres, B., Weber, H. I., 2018. “Numerical application of a stick-slip control and experimental analysis using a test rig.” In: MATEC Web of Conferences. vol. 148, p. 16009. EDP Sciences.

Pires, I., 2019. “Torsional FrictionInduced Vibrations in Slender Rotating Structures”. Master’s Thesis, Department of Mechanical Engineering, Pontifical Catholic University of Rio de Janeiro. Rio de Janeiro, Brazil.

Mansor, Z., Zakaria M. Z., Nor, A. M., Saad, M. S., Ahmad, R., and Jamaluddin, H., 2017. “NARMAX model identification of a palm oil biodiesel engine using multi-objective optimization differential evolution.” 3rd Electronic and Green Materials International Conference.

8. RESPONSIBILITY NOTICE

The authors are the only responsible for the printed material included in this paper.